ISSN 1063-7788, Physics of Atomic Nuclei, 2017, Vol. 80, No. 4, pp. 666–678. © Pleiades Publishing, Ltd., 2017.
Original Russian Text © L.S. Novikov, E.N. Voronina, L.I. Galanina, N.P. Chirskaya, 2017, published in Yadernaya Fizika, 2017, Vol. 80, No. 4, pp. 354–367.

ELEMENTARY PARTICLES AND FIELDS
Theory

Application of Nuclear-Physics Methods in Space Materials Science

L. S. Novikov[1),2)*], E. N. Voronina[1)], L. I. Galanina[1)], and N. P. Chirskaya[1)]

Received December 9, 2016; in final form, February 7, 2017

Abstract—The brief history of the development of investigations at the Skobeltsyn Institute of Nuclear Physics, Moscow State University (SINP MSU) in the field of space materials science is outlined. A generalized scheme of a numerical simulation of the radiation impact on spacecraft materials and elements of spacecraft equipment is examined. The results obtained by solving some of the most important problems that modern space materials science should address in studying nuclear processes, the interaction of charged particles with matter, particle detection, the protection from ionizing radiation, and the impact of particles on nanostructures and nanomaterials are presented.

DOI: 10.1134/S1063778817040172

1. INTRODUCTION

The impact of electrons, protons, and heavier ions of energy in the range of about 10^{-1} and 10^{14} MeV on spacecraft materials and elements of spacecraft equipment is one of the main reasons behind the degradation of reliability of spacecraft and the reduction of their working lifespan. Therefore, much attention has been given throughout the cosmic era to studying physical mechanisms of changes in the properties of spacecraft materials exposed to flows of charged particles [1, 2]. Soon after the discovery of the the Earth's radiation belts [1–3] by Soviet and American physicists in 1957 and 1958, there appeared experimental data compellingly proving a strong reduction of the efficiency of spacecraft solar batteries under the impact of particles from the Earth's radiation belts, as well as some other data suggesting a severe radiation damage of spacecraft materials and elements of spacecraft equipment [2, 4]. This gave a strong impetus to initiating large-scale work aimed at studying the radiation impact of space corpuscular radiation on spacecraft materials and at developing methods for the improvement of the strength of materials against this impact. Vigorous research work in these field, which was fostered by the needs of rapidly developing space technologies, led in fact to the creation of a new line of research—space materials science, whose tasks include, in addition to studying the radiation impact on spacecraft materials, investigations of effects caused by other space environment components, including plasma, solar electromagnetic radiation, and space debris and meteoroids [5, 6].

Space electron and ion flows whose energies lie in the above broad range are different in origin and in spatial and time characteristics. In the Earth's magnetosphere, defined by convention as the region of geomagnetic-field localization, the strongest radiation impact on spacecraft is exerted by particles of the Earth's radiation belts—that is, electrons, protons, and heavier ions captured by the geomagnetic field, their characteristic energies ranging between about 10^{-1} and 10^2 MeV. The lower boundary of the Earth's radiation belts lies above a larger part of the Earth's surface at an altitude of 10^3–1.5×10^3 km, while the maximum altitude of the upper boundary in the equatorial plane is about 50×10^3 km.

Solar energetic particles (SEP) and galactic cosmic rays (GCR) are dominant components of space radiation beyond the magnetosphere. SEP (mainly protons) of energy about 1 MeV to 10^4 MeV originate from the Sun in the period of intense bursts, while GCR are an isotropic flow of protons and heavier nuclei having energies in the range of 10^2–10^{14} MeV and coming from remote regions of the Milky Way Galaxy or from regions outside it [7]. The penetration of SEP and GCR particles into the magnetosphere is hindered by the screening effect of the geomagnetic field. Nevertheless, these particles can make a sizable contribution to the total radiation impact on spacecraft within the magnetosphere inclusive.

At the Skobeltsyn Institute of Nuclear Physics at Moscow State University (SINP MSU), investiga-

[1)]Skobeltsyn Institute of Nuclear Physics, Lomonosov Moscow State University, Moscow, 119991 Russia.
[2)]National Research University Higher School of Economics, ul. Myasnitskaya 20, Moscow, 101000 Russia.
[*]E-mail: novikov@sinp.msu.ru

tions into the impact of charged particles on materials used in space technologies have been performed since the early 1960s and were initiated by Academician S.N. Vernov, director of this institute at that time, who was involved in the studies resulting in the discovery of the Earth's radiation belts. A substantial contribution to the startup and development of these investigations was also due to I.B. Teplov [8], who headed the institute later, and to A.I. Akishin [5], who was the organizer and the first head of the Laboratory for Space Materials Science, which was created at the institute in 1985. As early as the late 1960s, highly important results recognized worldwide were obtained at SINP MSU in this field of research, which was new at that time.

By no means was the success of those studies in space materials science at SINP MSU accidental. To the early 1960s, a rather broad experience in performing experimental, as well as theoretical and computational, studies in various realms of nuclear and atomic physics had been gained at the institute. Moreover, the institute boasted a team of highly qualified specialists and possessed a number of ion and electron accelerators; last but not least, it was among the first laboratories in the Soviet Union that began studying physical conditions in space by means of instruments mounted on board spacecraft [1–4]. This circumstance was of great importance since, in the infancy of studies in space materials science, scientists and design engineers had to rely on rather scanty information about the properties of the space medium. New information obtained from the onboard equipment of spacecraft enabled considerable advances toward solving problems associated with ensuring the durability of spacecraft materials and elements of spacecraft equipment to the impact of this medium.

Thus, space research developed in parallel with studies in space materials science at SINP MSU and supplemented each other. Concurrently, methods that had much in common for these two research directions were developed for performing laboratory experiments and experiments on board spacecraft, along with mathematical-simulation methods relying on experimental and theoretical approaches referring not only to a direct investigation of nuclear processes but also to studies on the propagation of charged particles through matter, particle detection, and the protection from ionizing radiation.

In this article, we consider some of the most important problems in space materials science that are being presently solved at SINP MSU by means of nuclear-physics methods.

2. GENERALIZED SCHEME OF A SIMULATION OF THE RADIATION IMPACT ON SPACECRAFT MATERIALS AND ELEMENTS OF SPACECRAFT EQUIPMENT

At the present stage of the development of space materials science, a mathematical simulation of processes induced in matter by external effects is of paramount importance. The potential of available computer facilities and the state-of-the-art in methods for mathematical simulations permit performing calculations in which one can preset almost any features of external effects—for example, the energy and spatial distributions of charged particle flows incident to the object under study. Within models for respective computations, one can readily vary the composition and structure of materials under study, determine the character of coupling between processes proceeding in materials, preset the required time intervals, and so on. Such an approach makes it possible to study synergetic effects arising in response to the concerted action of various factors on the object under study and attracting a great deal of attention at the present time. At MSU, involved computational problems of space materials science are being solved on the basis of available supercomputers, including the "Lomonosov" supercomputer of speed about 900 Tflops, which is the most powerful of them.

On the basis of a comparative analysis of modern software and the computational methods used, the present authors developed a generalized scheme for simulating the radiation impact on spacecraft materials and elements of spacecraft equipment, employing computer codes extensively applied worldwide (see Fig. 1). This scheme takes into account structural features of typical elements of the framework and equipment used in modern spacecraft, as well as special features of the energy and spatial distributions of space radiation.

The FLUKA [9], GEANT3 [10], and GEANT4 [11] code packages based on the use of the Monte Carlo method and detailed models of radiation interaction with matter over a very broad energy range and shown in the central part of Fig. 1 have the highest potential. These codes make it possible to perform calculations for geometric structures arbitrarily specified by the user and subjected to the impact of electrons, ions that have various masses and charges, and a broad set of other particles. Presently, the GEANT3 code package is used quite rarely, since it is no longer upgraded. Moreover, it requires employing outdated software and its potential is substantially inferior to the potential of the more recently developed codes GEANT4 and FLUKA, which are being constantly upgraded further.

The spatial accuracy of calculations in the propagation of particles through matter is determined by

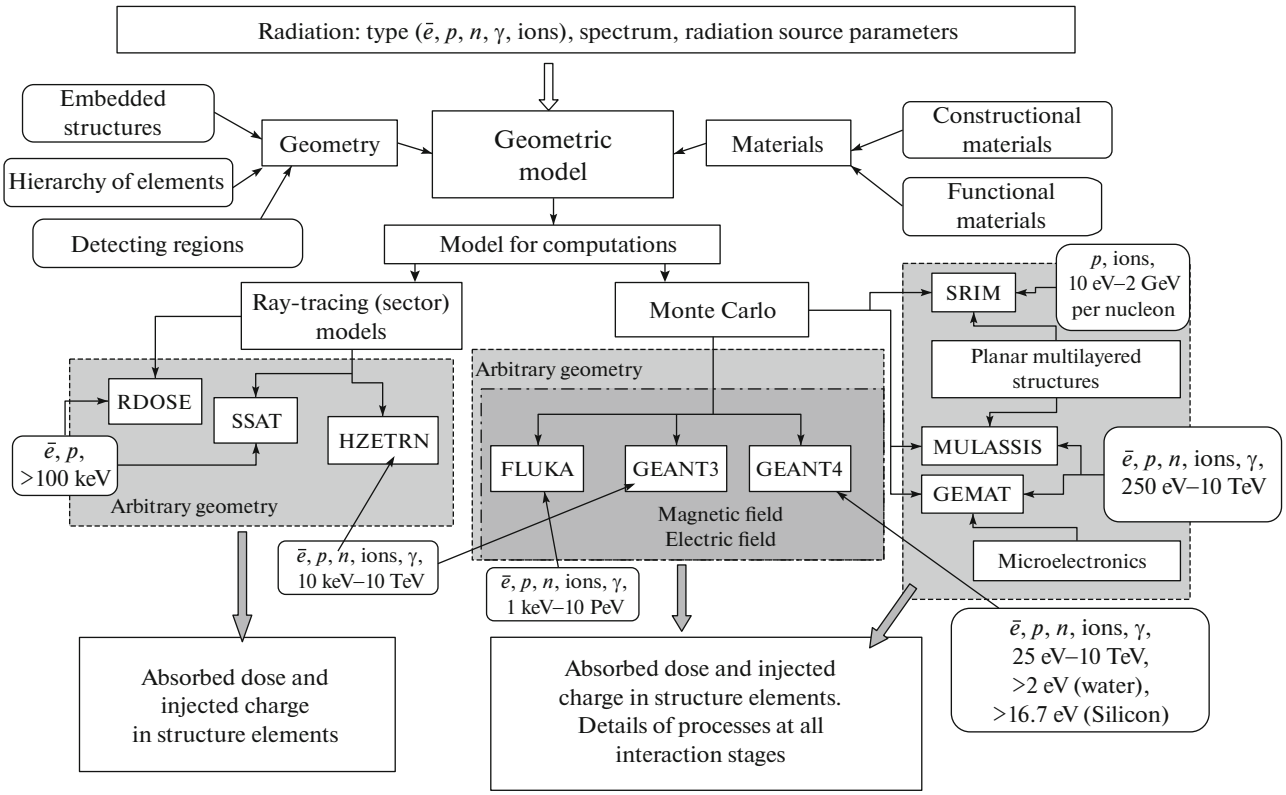

Fig. 1. Generalized scheme of a numerical simulation of the radiation impact on spacecraft materials by means of modern computer codes.

the minimum energy of electrons produced in the objects being studied that is accessible to simulations and which, in standard GEANT4 libraries, is 250 eV for the majority of materials.

The MicroElec library of electromagnetic interactions was created in order to study processes induced by radiation interaction with microelectronics elements. This library describes the deceleration in silicon of protons and heavier ions with energies of 50 keV per nucleon to 1 GeV per nucleon and electrons with energies of 16.7 eV to 100 MeV [12]. Secondary electrons are traced down to an energy of 5 eV [13, 14]. As a result, the spacial accuracy of the simulation in silicon is about 10 nm for heavy-ion tracks and about 1 μm for electron and light-ion tracks.

The FLUKA code is intended primarily for solving problems in high-energy and nuclear physics, but it is also widely used to simulate the propagation of particles through matter. In this code, the minimum energy of secondary electrons is 1 keV, which is somewhat above that in the GEANT4 code.

More narrowly specialized codes for solving standard engineering problems are presented in the right-hand part of the scheme (Fig. 1). Specifically, these are the MULASSIS [15], GEMAT [16], and SRIM [17] codes, which rely on the Monte Carlo method. They permit taking advantage of a rather simple geometry of the model for computations and obtaining a limited set of output data; however, the simplicity of employing them compensates for their drawbacks indicated here.

The SRIM/TRIM (Stopping and Range of Ions in Matter) code package is intended for simulating the motion of ions with energies in the range of 10^{-6}–2 GeV per nucleon in matter on the basis of the semiempirical interaction potential and with allowance for Coulomb screening [17]. Owing to the use of parameters determined on the basis of an analysis of vast sets of experimental data, SRIM permits taking into account the chemical structure of the material under study. In contrast to the GEANT code, SRIM is unable to analyze processes involving the production of secondary particles. Respective simulations may provide, among other things, spatial distributions of ions and displaced atoms, distributions of the energy loss by ionization and the total energy loss, and distributions of vacancies formed. The SRIM code is frequently used to solve nuclear-physics problems, but a small number of available geometry versions restricts severely its applicability region. The energy ranges of application of the FLUKA, GEANT4, and SRIM code packages are illustrated in Fig. 2.

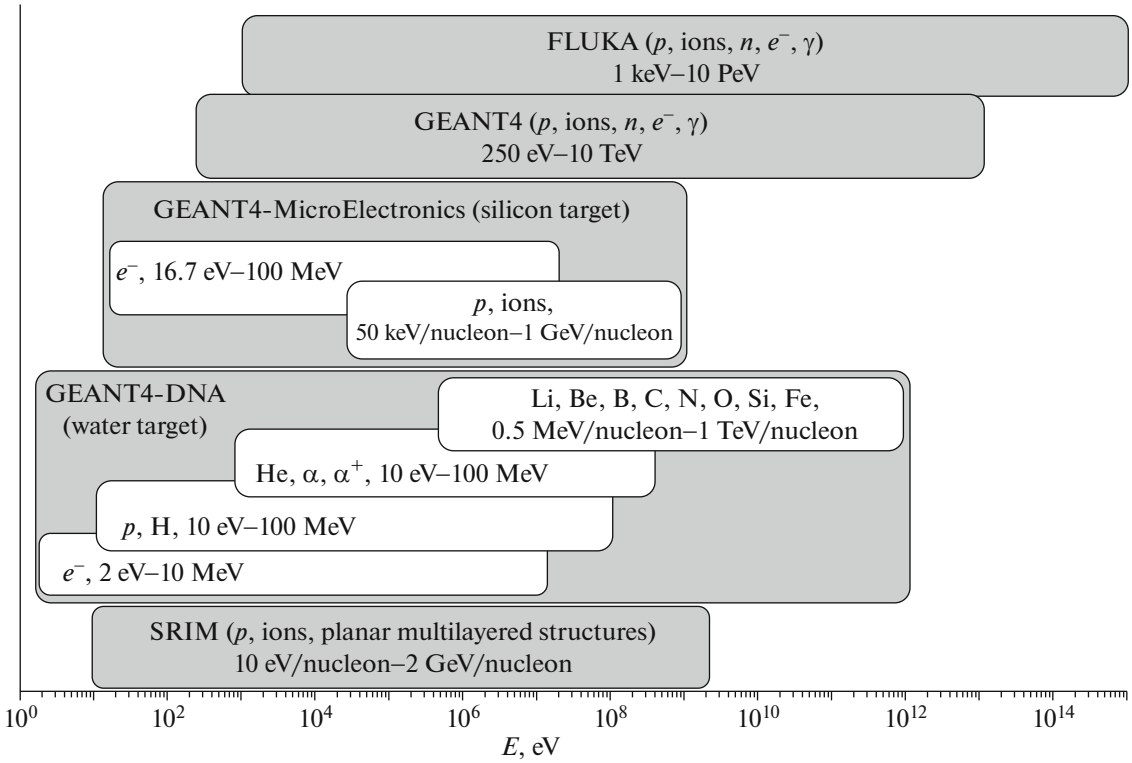

Fig. 2. Energy ranges of application of the FLUKA, GEANT4, and SRIM code packages.

The SRIM, FLUKA, and GEANT4 codes take no account of the change in the material structure in the course of irradiation—that is, effects associated with the accumulation of the absorbed dose. As a result, the incident-particle penetration depth may prove to be overestimated. The effects in question are taken into account within the TRIDYN code [18], which was developed on the basis of the SRIM algorithm and which is intended for simulating the impact of relatively heavy ions that have energies in the range of 10^{-2}–25 keV per nucleon.

Presented in the left-hand part of Fig. 1 are the RDOSE [19], SSAT [20], and HZETRN [21] codes whose computational algorithms are based on the ray-tracing (sector) method, within which the deceleration of individual particles in matter is not simulated, unlike in the Monte Carlo method; instead, the equivalent thickness of the protecting screen along the ray drawn from the point for which the computations are performed to an elementary area of the surface to which the particle flux is incident is calculated, whereupon the parameters of the radiation reaching the point in question are determined via the integration of the resulting angular distribution of equivalent protection thicknesses. Programs from this group are usually used in engineering calculations of the absorbed dose or electrical charge for the cases where there is no need for detailed information about individual events of particle interaction with matter.

3. RADIATION-INDUCED UPSETS IN MICROELECTRONICS ELEMENTS UNDER THE IMPACT OF SINGLE CHARGED PARTICLES

At the present time, radiation effects caused by individual charged particles are the most critical for the performance of spacecraft-microelectronics elements [22]. There are several kinds of such effects, which may be either reversible or irreversible, but, most frequently, there arise reversible single upsets; in this section, we consider physics mechanisms of their emergence.

Paradoxically as it may seem, the appearance of this problem was due to a technological advances in microelectronics. In modern integrated circuits, characterized by a high degree of integration, electrical charges that control their performance proved to be commensurate with charges that arise in the microcircuit material upon the propagation of particles (heavy nuclei from GCR or protons from the Earth's radiation belts) that are able to initiate nuclear reactions in this material. The motion of these induced electric charges in the electric fields within a microcircuit is the reason for the occurrence of the aforementioned upsets.

Thus, a single event upset occurs when the charge arising upon the decelerated-particle-induced ionization of atoms of the microcircuit material reaches a

value Q_0 that is critical for microelectronics elements (transistors) and which one can use as a criterion of the emergence of single upsets. This charge is related to the threshold energy deposition by the equation $E_0 = \varepsilon Q_0/q$, where ε is the energy spent on the production of one electron–hole pair and q is an elementary charge. Quite an efficient accumulation of the product charge by the microcircuit electrodes is yet another important condition of the emergence of single upsets. Therefore, this charge should be produced within some bounded region.

The creations of a charge in microcircuit matter by space radiation particles, with the result that single upsets occur, is due to two physics mechanisms. The first consists in the direct ionization of atoms by heavy ions ($Z > 10$) from GCR, while the second is their ionization induced by recoil nuclei and particles originating from nuclear interaction of protons and light ions from the Earth's radiation belts and SEP [23] with matter at energies of incident particles from 30 to 40 MeV.

For modern integrated microcircuits, in which the linear dimensions of active elements are close to 0.1 μm, $Q_0 \sim 10^{-13}$ C, while the E_0 value corresponding to this charge is 5 to 30 MeV for various elements.

The charge created in microcircuit matter via the direct ionization of atoms by a heavy ion from GCR can be estimated by means of the aforementioned code packages based on the Monte Carlo method.

Here, we will consider the mechanism of charge creation by nuclear-reaction products; in order to analyze this mechanism, which has not yet received sufficient study, it is necessary to know the cross sections for the nuclear interaction of incident particles with matter [24–26]. Their values are either determined on the basis of available databases [27, 28] or calculated within various theoretical approaches. In technical applications, use is also made of phenomenological approximations [29]. Unfortunately, the present-day experimental database of cross sections for the nuclear interaction [27, 28] of ions with nuclei of silicon (^{28}Si), which we will consider as the main component of the microcircuit material, is quite scanty for the range of energies in the Earth's radiation belts; moreover, there is no complete and consistent model of nuclear reactions.

We note that, by means of the GEANT3, GEANT4, and FLUKA code packages presented in Fig. 1, one can in general calculate the charge created by a decelerated particle, taking into account ionization induced by recoil nuclei and secondary particles. However, the results of such simulations are ambiguous and depend on the choice of nuclear-reaction model.

The nuclear-interaction cross sections presented here were calculated on the basis of the exciton model of the compound nucleus for energies not higher than 30 MeV [30, 31] and on the basis of the HMS preequilibrium exciton model for higher energies [32]. The application of the models in question was accomplished by embedding them into the EMPIRE code package [33]. The viability of these models was confirmed by an analysis of the results of measurements at the SINP MSU cyclotron the angular characteristics of elastic scattering of 30.3-MeV alpha particles by ^{28}Si nuclei and their inelastic scattering by these nuclei that is accompanied by the excitation of their three lowest levels [30].

In general, the frequency of single upsets at an instant t depends on the differential flux $\Phi_i(E)$ of incident ions belonging to an i type and having an energy E and on $\sigma_i(E, E_0)$, which is the macroscopic cross section for a single upset whose threshold energy is E_0, [22]; that is,

$$\nu(t, E_0) = \sum_i \int \Phi_i(E)\sigma_i(E, E_0)dE.$$

The macroscopic cross section $\sigma_i(E,\ E_0)$ for a single upset caused by nuclear interactions is determined by the number of atoms in the sensitive volume of the microcircuit, N, and the sum of the cross sections for the production of recoil nuclei with energy E_r over all nuclear-reaction channels k; that is,

$$\sigma_i(E, E_0) = N \sum_k \int\limits_{E_0} \frac{d\sigma_i^k(E, E_r)}{dE_r} dE_r.$$

The original calculated value is the differential cross section $\frac{d\sigma_i^k(E,E_r)}{dE_r}$ for the production of nuclei with mass A, charge Z, and energy E_r in the interaction of primary i type ions with E energy at a nucleus of the microcircuit material.

Figure 3 shows the calculated dependences of the total cross sections $\sigma_i^k(E, E_r) = \int \frac{d\sigma_i^k(E,E_r)}{dE_r} dE_r$ on the energy of incident protons interacting with (Fig. 3*a*) ^{28}Si and (Fig. 3*b*) ^{12}C nuclei. One can see that the reactions leading to the production of the isotopes ^{26,27}Al and ^{27}Si are the most probable in the first case. The process in which a ^{24}Mg nucleus is produced via the separation of an alpha particle also has a high probability. The contribution of elastic and quasielastic collisions is significant at proton energies below 30 MeV and becomes smaller as this energy grows. Carbon and boron isotopes are primarily produced in the second case. Also, scattering processes remain dominant up to an energy of about 60 MeV in that case.

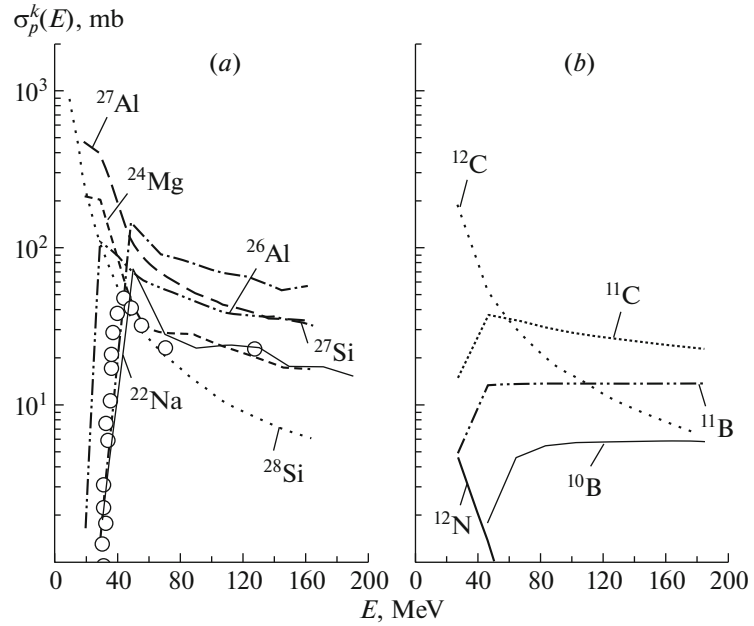

Fig. 3. Cross sections for the production of recoil nuclei versus the primary proton energy for the (*a*) $p + {}^{28}$Si (the displayed points represent the experimental cross sections for the production of a ^{22}Na nucleus in the $p + {}^{27}$Al reaction [29] along with their calculated counterparts) and (*b*) $p + {}^{12}$C reactions.

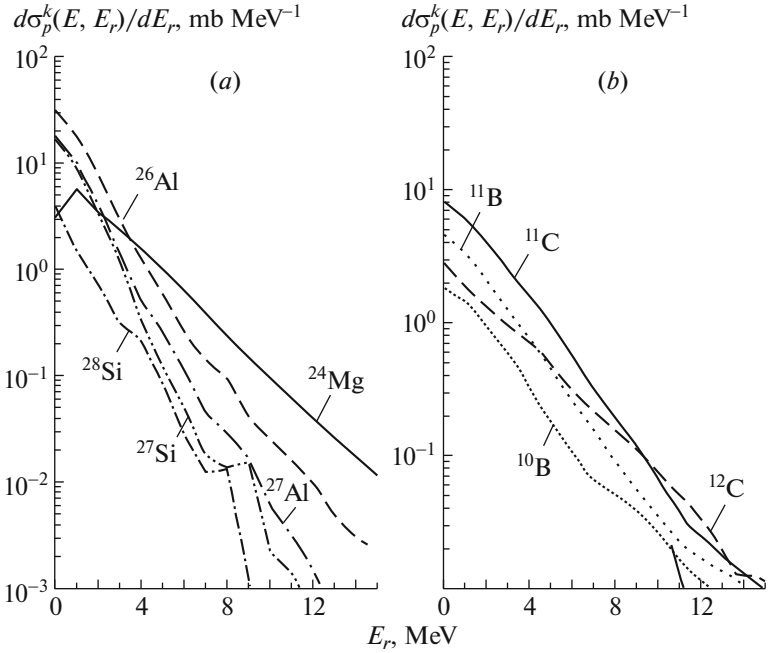

Fig. 4. Energy spectra of recoil nuclei from the interaction of $E = 150$ MeV protons with (*a*) ^{28}Si and (*b*) ^{12}C nuclei.

The energy spectra of the most probable recoil nuclei are given in Fig. 4 according to the calculation at the incident-proton energy of $E = 150$ MeV. One can see that the cross sections in question decrease almost exponentially as the energy recoil nuclei grows and that there is no correlation between the exponent index and the mass number of recoil nuclei.

The quoted data make it possible to calculate, on the basis of the expressions presented above, the frequency of single upsets in microcircuits because of the occurrence of nuclear reactions. Such calculations are of importance, for example, in estimating the potential of new probing equipment based on powerful femtosecond lasers [23].

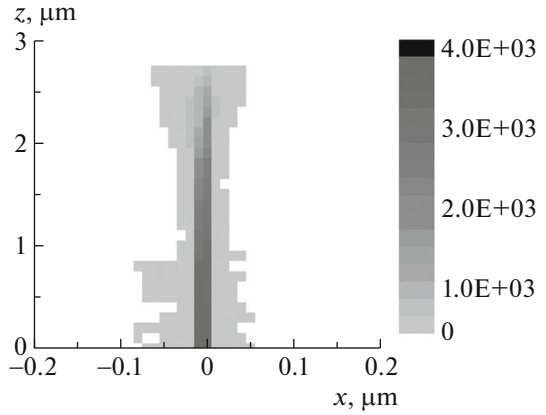

Fig. 5. Averaged distribution of the charge in the longitudinal section (z, x) of the track of deceleration of a 15-MeV ^{27}Al nucleus in a silicon microvolume (the charge-density scale is given in electron-charge units).

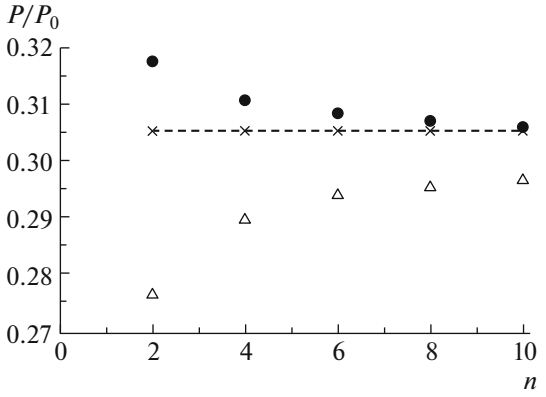

Fig. 6. Relative flux P/P_0 of energy of protons that traversed a screen 100 μm in thickness as a function of the number n of alternating W and Al layers for different orders of alternation of the materials: (closed symbols) W/Al and (open symbols) Al/W. The dashed line going through crosses corresponds to a uniform screen having the equivalent chemical composition and density.

It was indicated above that, for the occurrence of a single upset, it is important that the accumulation of the charge by the microcircuit electrodes that is created by a decelerated particle in the microcircuit volume was nearly complete. In order to estimate the dimensions of emerging deceleration tracks, the deceleration in silicon of a ^{27}Al recoil nucleus with an energy of 15 MeV and an alpha particle with the same energy was simulated by means of the GEANT4 code. Figure 5 gives the results obtained by calculating the distribution of the averaged charge over the track of the deceleration of a ^{27}Al nucleus in a silicon target. The integrated charge that was generated in that case was 2.3×10^{-14} C. For the sake of comparison, we have calculated the integrated charge that was created in the same volume by a decelerated alpha particle, even though its range before a full stop is longer than the length over which the computations are performed. In the latter case, the charge proved to be 2.3×10^{-17} C. These charge values, which are consistent with the values presented above for the critical charge Q_0, show that it is predominantly the recoil nuclei that create the charge in silicon.

4. EFFICIENCY OF RADIATION-PROTECTION SCREENS AND CHARGED-PARTICLE DETECTORS

In order to accomplish the protection from the ionizing radiation impact, one can employ homogeneous and heterogeneous screens characterized, in particular, by the chemical composition of the materials used in them and by relative positions of their structural element. The Monte Carlo approaches in Fig. 1 to numerically simulating the interaction of charged particles with matter make it possible to optimize radiation protective screens by varying the above characteristics.

The possibility of creating multilayered screens consisting of alternating layers that have different chemical compositions is being vigorously studied at the present time. The order of layers from materials that have different physical properties and their thickness play a significant role for such screens in attenuating the flux of incident ionizing radiation. By way of example, the relative flux of the energy of protons that traversed multilayered screens from alternating layers of tungsten (W) and aluminum (Al) is shown in Fig. 6 as a function of the number n of alternating layers according to calculations performed by means of the GEANT4 code package for the primary proton energy of 6 MeV [34]. The total screen thickness (50 μm of Al plus 50 μm of W) remained unchanged. Upon an increase in the number of alternating layers, the parameters of the multilayered screen become closer to the parameters of the homogeneous screen that has the equivalent average chemical composition and density (dashed line in Fig. 6).

The above result is explained on the basis of an analysis of special features of the processes of incident proton deceleration and backscattering in light- (Al) and heavy-metal (W) layers. Upon the change in the order of layers manufactured from the different materials, the energy and angular distributions of charged particles penetrating into the successive layer change substantially. The results of the calculations also reveal that, in employing the above materials, an increase in the number of layers does not improve the efficiency of the screens.

The problem of protecting spacecraft materials and elements of spacecraft equipment from the impact of ionizing radiation is of importance not only

Fig. 7. Discharge channels in a glass sample after the irradiation of it with a flux of 1-MeV electrons.

from the point of view of the accumulation of the absorbed dose in the elements being considered but also from the point of view of the electric charge accumulation in the volume of the dielectric material.

High-frequency electron accelerators created at SINP MSU and rated to the electron energies of 1 and 10 MeV [35], which correspond to the energies of the electrons from the Earth's radiation belts, are successfully used to study experimentally the accumulation of the absorbed dose in materials and the formation of the induced charge. The impact of electrons from the Earth's radiation belts on the materials under study is simulated correctly under laboratory conditions by arranging properly shaped scatterers of various configurations in front of the samples of these materials. Owing to these scatterers, a monoenergetic electron flow extracted from an accelerator is transformed into an electron flow whose energy spectrum is characteristic of electrons from the Earth's radiation belts. The scatterer configuration and thickness are chosen on the basis of the results of a numerical Monte Carlo simulation of electron propagation through the scatterer under study.

The conditions for the emergence of space discharges are considered in studying the accumulation of the product charge. If the strength of the electric field created by the product charge exceeds the material electric strength, an electric discharge arises within it, leading to the formation of a characteristic figure frequently referred to as a Lichtenberg figure [36]. A figure of this type that was obtained upon exposing a glass sample to a flow of 1-MeV electrons at the SINP MSU accelerator is shown in Fig. 7. The central discharge channel goes to one of the faces of the irradiated sample, while the side channels arise because of the destruction of the dielectric material by electrons moving to the central channel.

A numerical simulation of processes induced by the interaction of charged particles with matter is also used successfully in studying detectors applied in space technologies or in laboratory investigations.

Usually, the energy loss of particles in detectors is determined by means of analytic calculations on the basis of available data on the linear loss of particle energy in matter. Respective calculations revealed that this method is quite acceptable in detecting protons and heavier ions but leads to large errors in detecting electrons. In view of this, we have proposed a method for calculations that relies on directly examining the electron-detection efficiency defined as the ratio of the number N of electrons recorded by the detector under study to the total number N_0 of incident electrons [37]. This approach permits correctly taking into account the spread of the electron energy loss in the detector material.

We have examined a telescopic detecting system that consists of two silicon semiconductor detectors 0.3 and 1.6 mm in thickness arranged in series and separated by an aluminum absorber 0.6 mm thick. For each detector, one sets a threshold energy that determines the boundaries of the energy range for detected particles.

Figure 8*a* shows the results of the calculations performed by means of the GEANT4 code package for the efficiency of isotropic electron flow detection in the first ($D1$, solid curves) and second ($D2$, dashed curves) detectors of the telescopic system for various values of the incident electron energy and threshold energy E_{thr}. Figure 8*b* gives a three-dimensional picture of the full metrological characteristic of the telescopic detecting system in the form of the dependence of the detection efficiency for electrons on their energy E and on the threshold energy E_{thr}.

The procedure outlined above makes it possible to improve the accuracy in measuring flows of electrons in space and to choose parameters of detecting systems for specific problems.

4.1. Interaction of Corpuscular Radiation with Nanostructures and Nanomaterials

By nanostructured materials (nanomaterials), one usually means materials consisting of structural elements of various configuration like particles (grains), fibers, tubes, and films for which at least one linear dimension lies in the range of $1-10^2$ nm [38]. Nanomaterials may possess physical properties substantially better than those of conventional materials, and this permits creating, on their basis, equipment characterized by unique performance parameters and even sometimes employing new principles of operation of

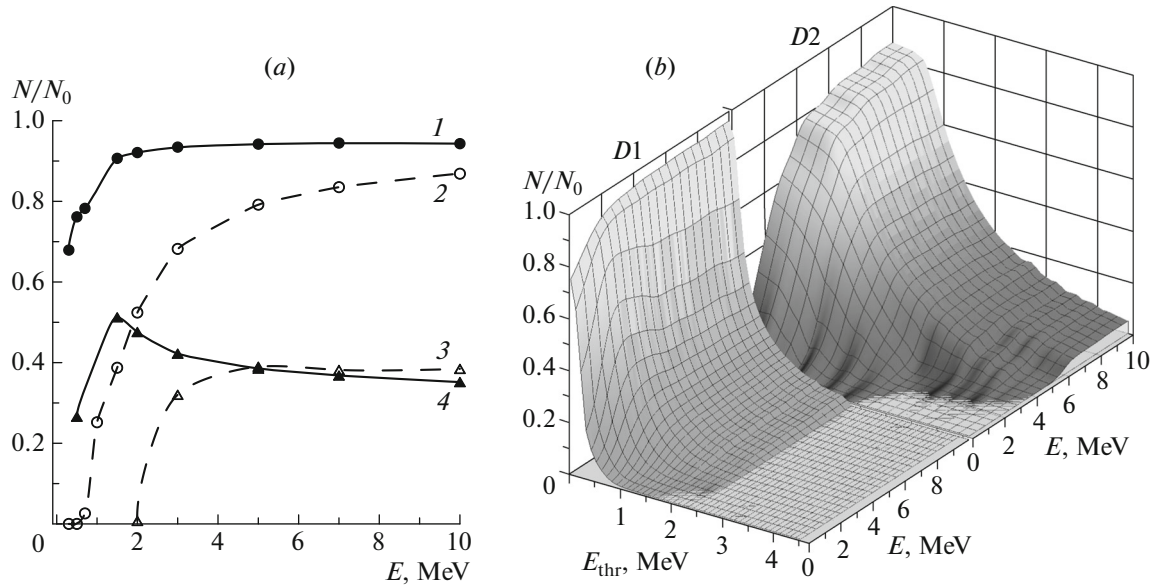

Fig. 8. (*a*) Detection efficiency for electrons of various energies in the (solid curves and close symbols) first and (dashed curves and open symbols) second detectors at the threshold energy values of (curves *1* and *2*) 0.1, (*3*) 1.5, and (*4*) 0.4 MeV. (*b*) Metrological characteristic of the detecting system.

designed devices. A substantial improvement of the properties of nanomaterials is due to the size effects, which one can describe within classical or quantum-mechanical approaches [39–43].

Radiation effects arising under the action of ionizing radiation in nanostructures and materials created on their basis have some special features in relation to similar effects in objects whose dimensions lie in micro and macro ranges [44–48]. In the case where an electron or an ion of rather high energy characteristic of space radiation interacts with a nanostructure, only a very small part of the incident-particle energy is transferred to a nanosized object, with the result that, in it, there arises a very small number of additional charge carriers or structural defects. As the incident-particle energy grows, the number of arising charge carriers and defects decreases in accordance with the decrease in the cross section for interaction with atoms of the material [44, 49]. Usually, nanostructures are characterized by a small number of defects [44], and this is explained to a considerable extent by their ability to heal defects via a fast rearrangement of interatomic bonds [40]. The decrease in the number of radiation defects is also due to the circumstance that displaced atoms have wider possibilities for leaving the nanostructure owing to a large ratio of its surface area to its volume [50].

The processes of migration of radiation defects in traditional and nanostructured materials are substantially different. In nanostructured materials, which consist of a large number of nanosized grains, displaced atoms go out from the grain volume to the grain boundaries, where they are pinned. After capture at the boundaries, the atoms may be injected into the interior of grains, where they undergo recombination with available vacancies. As a result, an efficient mechanism of drain of displaced atoms to these surfaces is operative in nanostructured materials, and this mechanism hinders the accumulation of radiation defects in the grain volume [45].

Thus, processes leading to the formation of charge carriers and structural defects in nanostructured materials have some important features distinguishing them from respective processes in ordinary materials.

In simulating the radiation impact on nanostructured materials, it is necessary to employ so-called multiscale simulation based on the application of some set of computational methods dealing with different spatial and time scales—from quantum-mechanical methods based on numerically integrating the equations of quantum mechanics to continuum mechanics used to analyze macroscopic objects [51].

The formation and migration of point and small topological defects in nanostructures are studied by quantum-mechanical methods based on the classic Hartree–Fock approach, which is extensively used to determine the structure of atomic nuclei [52]. For periodic structures, one applies the method of density functional theory (DFT) [53]. This method is applied to calculating the electron structure of heavy nuclei [54]. By employing the DFT method, one calculates the parameters of defects in solids and simulates processes induced by the interaction of fast

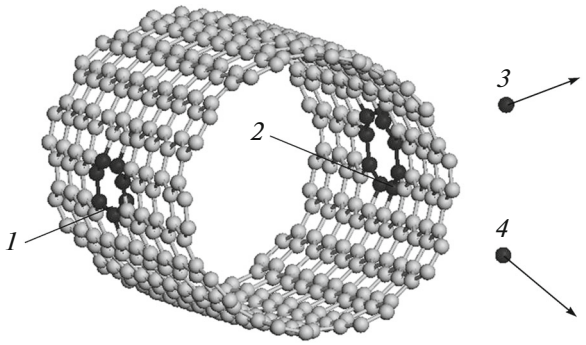

Fig. 9. Formation of vacancies in a carbon nanotube upon the interaction with a hydrogen atom (for explanations, see main body of the text).

atoms with nanostructures [44, 46]. A semiempirical method of density functional based tight-binding (DFTB) was developed in order to simulate more complex schemes. In this approach, a parametrization based on ab initio calculations is used [55].

The method of molecular dynamics (MD), within which the interaction of atoms is described in terms of empirical potentials or force fields, is widely used to simulate cascade processes. Owing to a number of modifications [44], this method makes it possible to simulate the displacement and knockout of atoms from lattice nodes, their recombination with emerging vacancies, and the formation of disordered clusters of defects, as well as to study the formation of tracks of high-energy particles [50].

Figure 9 shows the results obtained from a DFTB simulation of the knockout of carbon atoms from the walls of a carbon nanotube by an incident hydrogen atom [56]. In this case, the incident atom has created a vacancy in the front wall of the carbon nanotube (*1*) by knocking out a carbon atom (*3*), which escapes thereupon from the nanotube. The formation of the second vacancy (*2*) is due to a displaced carbon atom (*3*) that, upon a collision event, receives an energy that is sufficient for knocking out yet another carbon atom (*4*).

The mathematical-simulation methods outlined above can successfully be used to describe the interaction of nanostructures with low-energy atoms. The sputtering of polymer materials by atomic oxygen, which is the main component of the Earth's upper atmosphere at altitudes in the range of 200–800 km, is an important problem in space materials science. The chemical activity of atomic oxygen is enhanced owing to the spacecraft orbital velocity, via which a kinetic energy of about 5 eV is transferred to atoms upon their collisions with the spacecraft surface. In the majority of cases, chemical sputtering of the material surface leads to erosion accompanied by the release of volatile reaction products, whereby the loss of the material mass occurs [57, 58]. The erosion of materials may lead to the degradation of not only their mechanical strength but also many other physicochemical properties.

The impact of atomic oxygen on massive samples of vertically oriented carbon nanotubes 20 to 100 nm in diameter obtained at SINP MSU by the method of pyrolytic gas-phase precipitation [59] was studied at the SINP MSU magnetoplasmadynamic accelerator, which makes it possible to form flows of fast neutral and ionized oxygen atoms with an average energy of about 20 eV [58].

Figure 10*a* shows the destruction of an array of carbon nanotubes at fluence values in excess of 5×10^{19} cm^{-2} [60]. The so-called "fluffing" of nanotubes, which proceeds most vigorously near their tips, is characteristic feature of the destruction [61]. Figure 10*b* shows the results obtained from a simulation of the destruction of nanotubes by the DFT method. Upon the impact of oxygen atoms, side nanotube walls split into thin strips, which are fragments of graphene nanoribbons. There are reasons to assume that the aforementioned fluffing out is intimately related to the well-known phenomenon of unzipping of carbon nanotubes [62, 63].

A code for calculating the chemical spraying of polymer materials was developed at SINP MSU on the basis of the GEANT3 code package [64]. In the respective model for computations, one breaks down the material under study into equal-sized cells and, as impacting objects, uses enlarged particles in the form of a conglomerate of a rather large number of neutral oxygen atom. The number of oxygen atoms per enlarged particle, the cell size, and probabilities for processes of particle interaction with cells are chosen on the basis of experimental data.

The impact of an atomic-oxygen flow on a polymeric composite material in the form of a polymer matrix in which spherical particles stable to the impact of oxygen atoms were introduced was simulated. As fillers, we can consider nanosized particles, but, because of an excess surface energy, they tend to form agglomerates whose size may exceed substantially their original diameter and reach several micrometers and which depends on the degree of dispersion [40]. In the course of irradiation with an oxygen plasma, filler particles play the role of a screen that protects the lower lying polymer from the impact of oxygen atoms. The efficiency of this screening depends not only on the properties of these particles but also on their size [64].

Figure 11*a* shows the picture that a scanning electron microscope gave for the surface of a polymeric composite material that was doped with nanosized silicon-oxide particles forming agglomerates

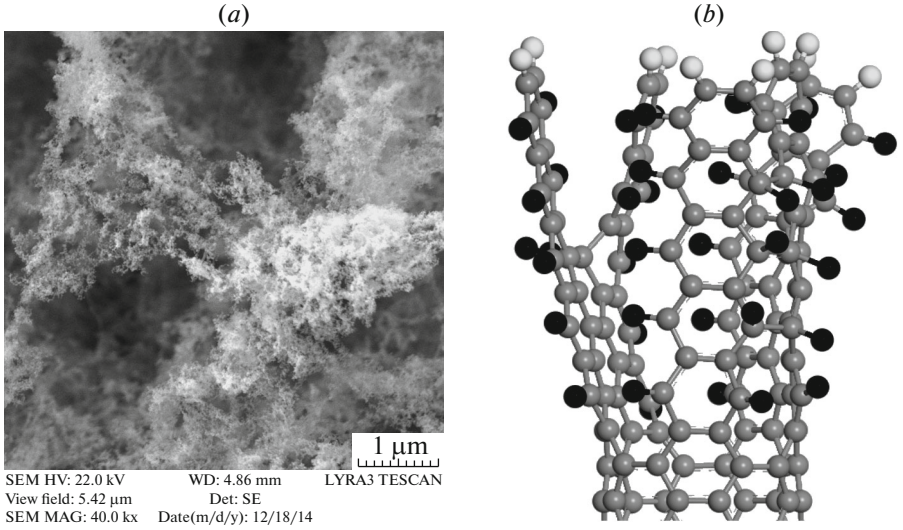

Fig. 10. (*a*) Picture of the carbon nanotube array surface irradiated with an oxygen plasma and (*b*) result of a simulation of this irradiation by the DFT method. The carbon, oxygen, and hydrogen atoms are represented by, respectively, gray, black, and white balls.

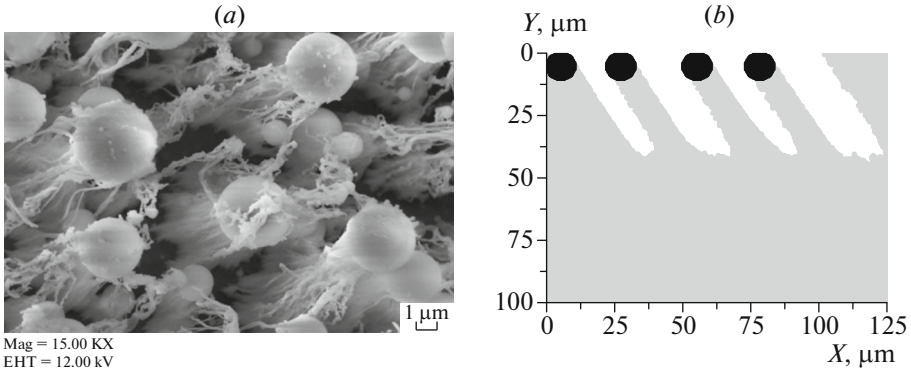

Fig. 11. (*a*) Structure of a polymeric composite material after its exposure to a flow of atomic oxygen and (*b*) results of the respective mathematical simulation.

and which was exposed thereupon to a flow of atomic oxygen. The results obtained by mathematically simulating the erosion of a polymer in which one row of spherical particles 10 μm in diameter was introduced in the surface layer are given in Fig. 11*b*.

As a quantitative measure of the stability of a material against the impact of atomic oxygen, one can employ the decrease in its volume or mass. The results obtained show that the introduction of silicon-oxide particles in a polymer matrix leads to the reduction of the mass loss for the resulting material by a factor of two to four in relation to the original polymer [65].

Investigation of the synergistic effect of external factors is an important problem in space materials science. The successive impact of flows of 0.5- and 7.5-MeV protons from the SINP MSU ion accelerators [49] and atomic oxygen on polymer films was studied at SINP MSU. The results showed that the preliminary creation of radiation defects in polymers by incident protons leads to an slight enhancement of chemical sputtering induced by atomic oxygen [66].

5. CONCLUSIONS

The results presented in this article have demonstrated a high efficiency of employing theoretical-computational and experimental methods of nuclear and atomic physics in solving important problems of space materials science. Owing to the use of these methods, we have obtained new data on nuclear interactions of space protons with materials of microelectronics elements, on protection from space ionizing radiation, on the detection of electrons and ions in space, and on special features of the impact of space radiation particles on nanostructures and nanomaterials. We have also demonstrated the

possibility of studying, by such methods, the impact that atomic oxygen, which exists in the near-Earth space, exerts on polymeric composite materials, as well as the combined effect of flows of oxygen atoms and protons on polymers. The new data obtained in this way are being employed in various fields of contemporary space materials science.

ACKNOWLEDGMENTS

This work was supported by the Russian Foundation for Basic Research (project no. 14-29-09244).

REFERENCES

1. S. N. Vernov, P. V. Vakulov, and Yu. I. Logachev, in *Achievements of USSR in the Study of Cosmic Space: First Ten Cosmic Years, 1957–1967, Collection of Articles* (Nauka, Moscow, 1968), p. 106 [in Russian].
2. L. S. Novikov and M. I. Panasyuk, Vopr. At. Nauki Tekh., Ser. Fiz. Rad. Vozdeistv. Radioelektron. Appar., No. 4, 3 (2002).
3. S. N. Vernov, N. L. Grigorov, Yu. I. Logachev, and A. E. Chudakov, Sov. Phys. Dokl. **3**, 617 (1958).
4. Yu. I. Logachev, *40 Years of Cosmic Era in SINPh MSU* (Mosk. Gos. Univ., Moscow, 1998) [in Russian].
5. A. I. Akishin and L. S. Novikov, in *Encyclopedy of Lomonosov Moscow State University. Skobeltsyn Institute of Nuclear Physics,* Collection of Articles (Biblion–Russkaya kniga, Moscow, 2006), p. 55 [in Russian].
6. L. S. Novikov, Moscow Univ. Phys. Bull. **65**, 259 (2010).
7. *Radiation Conditions in Cosmic Space,* Ed. by M. I. Panasyuk (Biblion–Russkaya kniga, Moscow, 2006), p. 132 [in Russian].
8. *Igor Borisovich Teplov: To 80th Anniversary of Birth,* Ed. by N. S. Zelenskaya, M. I. Panasyuk, and E. A. Romanovsky (Univ. Kniga, Moscow, 2008), p. 113 [in Russian].
9. T. T. Böhlen et al., At. Data Nucl. Data Sheets **120**, 211 (2014); A. Ferrari, P. R. Sala, A. Fasso, and J. Ranft, *FLUKA: a Multi-Particle Transport Code* (CERN, Geneva, 2005), INFN/TC_05/11, SLAC-R-773; http://www.fluka.org/fluka.php.
10. R. Brun et al., *GEANT. Detector Description and Simulation Tool. User's Guide* (CERN, Geneva, 1993).
11. S. Agostinelli et al., Nucl. Instrum. Methods Phys. Res. A **506**, 250 (2003).
12. https://twiki.cern.ch/twiki/bin/view/Geant4/LowEMuElec.
13. S. Incerti et al., Med. Phys. **37**, 4692 (2010).
14. Geant4 Physics Reference Manual, Version Geant4 10.1 (2014). http://geant4.web.cern.ch/geant4/UserDocumentation/UsersGuides/PhysicsReferenceManual/fo/PhysicsReferenceManual.pdf.
15. F. Lei et al., IEEE Trans. Nucl. Sci. **49**, 2788 (2002).
16. F. Lei and P. Truscott, *Geant4-Based Microdosimetry Analysis Tool. Software User's Manual* (QinetiQ, Farnborough, 2007).
17. J. F. Ziegler, M. D. Ziegler, and J. P. Biersack, Nucl. Instrum. Methods Phys. Res. B **268**, 1818 (2010).
18. W. Möller and W. Eckstein, Nucl. Instrum. Methods Phys. Res. B **2**, 814 (1984).
19. A. A. Makletsov, V. N. Mileev, L. S. Novikov, and V. V. Sinolits, Inzh. Ekol., No. 1, 39 (1997).
20. www.spenvis.oma.be/help/models/ssat.html.
21. J. L. Shinn and J. W. Wilson, NASA Technical Paper 3147 (NASA, 1992).
22. A. I. Chumakov, *Cosmic Radiation Effect on Integral Circuits* (Radio Svyaz', Moscow, 2004).
23. I. N. Tsymbalov, K. A. Ivanov, R. V. Volkov, A. B. Savel'ev, L. S. Novikov, L. I. Galanina, N. P. Chirskaya, V. Yu. Bychenkov, and A. I. Chumakov, Fiz. Khim. Obrab. Mater., No. 1, 25 (2016).
24. T. Bion and J. Bourrieau, IEEE Trans. Nucl. Sci. **36**, 2281 (1989).
25. A. Akkerman, J. Barak, and Y. Lifshitz, IEEE Trans. Nucl. Sci. **49**, 1539 (2002).
26. V. Andersen et al., Adv. Space Res. **34**, 1302 (2004).
27. http://www.nndc.bnl.gov/sigma/getInterpreted.jsp?evalid=10917&mf=6&mt=5.
28. ftp://ftp.nrg.eu/pub/www/talys/tendl2014/tendl2014.html.
29. N. V. Kuznetsov, Vopr. At. Nauki Tekh., Ser.: Fiz. Rad. Vozdeistv. Radioelektron. Appar., Nos. 1–2, 46 (2007).
30. E. N. Voronina, L. I. Galanina, N. S. Zelenskaya, V. M. Lebedev, V. N. Mileev, L. S. Novikov, V. V. Sinolits, and A. V. Spassky, Bull. Russ. Acad. Sci.: Phys. **73**, 197 (2009).
31. H. Nishioka, J. J. M. Verbaarschot, H. A. Weidenmüller, and S. Yoshida, Ann. Phys. (N. Y.) **172**, 67 (1986).
32. M. Blann and M. B. Chadwick, Phys. Rev. C **57**, 233 (1998).
33. http://www.nndc.bnl.gov/empire/.
34. E. N. Voronina and N. P. Chirskaya, Fiz. Khim. Obrab. Mater., No. 5, 23 (2013).
35. O V. Chubarov, A. S. Alimov, and V. I. Shvedunov, IEEE Trans. Nucl. Sci. **44**, 1037 (1997).
36. V. V. Gromov, *Electrical Charge in Irradiated Materials* (Energoizdat, Moscow, 1982) [in Russian].

37. N. A. Vlasova, L. S. Novikov, I. A. Rubinshtein, A. V. Spassky, and N. P. Chirskaya, Fiz. Khim. Obrab. Mater., No. 6, 32 (2013).
38. ISO/TS 27687: Nanotechnologies—Terminology and Definitions for Nano-Objects (2008).
39. *Nanoscale Science and Technology,* Ed. by R. W. Kelsall, I. W. Hamley, and M. Geoghegan (Wiley, Hoboken, NJ, 2005).
40. M. S. P. Shaffer and J. K. W. Sandler, *Processing and Properties of Nanocomposites* (World Scientific, Singapore, 2006), Chap. 1.
41. K. A. Watson and J. W. Connell, in *Carbon Nanotechnology: Recent Developments in Chemistry, Physics, Materials Science, and Device Applications,* Ed. by L. Dai (Elsevier, Amsterdam, 2006), p. 677.
42. I. P. Suzdalev, *Nanotechnology: Physicochemistry of Nanoclusters, Nanostructures and Nanomaterials,* 2nd ed. (Librokom, Moscow, 2009) [in Russian].
43. L. S. Novikov and E. N. Voronina, *Prospects of Nanomaterial Application in Cosmic Technology* (Universitetskaya kniga, Moscow, 2008) [in Russian].
44. A. V. Krasheninnikov and K. Nordlund, J. App. Phys. **107**, 071301 (2010).
45. G. Ackland, Science **327**, 1587 (2010).
46. Y. Zhang and W. J. Weber, in *Ion Beams in Nanoscience and Technology,* Ser. Particle Acceleration and Detection, Ed. by R. Hellborg et al. (Springer, Berlin, Heidelberg, 2009).
47. I. A. Ovid'ko and A. G. Sheinerman, Appl. Phys. A **81**, 1083 (2005).
48. R. A. Andrievskii, Phys. Met. Metallogr. **110**, 229 (2010).
49. L. S. Novikov, V. N. Mileev, E. N. Voronina, L. I. Galanina, A. A. Makletsov, and V. V. Sinolits, J. Surf. Invest.: X-Ray, Synchrotr., Neutron Tech. **3**, 199 (2009).
50. K. Nordlund and F. Djurabekova, J. Comput. Electron. **13**, 122 (2014).
51. R. B. Ross and S. Mohanty, *Multiscale Simulation Methods for Nanomaterials* (Wiley, Hoboken, 2008), Chap. 1.
52. M. Bender, P.-H. Heenen, and P.-G. Reinhard, Rev. Mod. Phys. **75**, 121 (2003).
53. P. Hohenberg and W. Kohn, Phys. Rev. B **136**, 864 (1964); W. Kohn and L. J. Sham, Phys. Rev. A **140**, 1133 (1965).
54. *Extended Density Functionals in Nuclear Structure Physics,* Ed. by G. A. Lalazissis, P. Ring, and D. Vretenar, Lect. Notes Phys. **641** (2004).
55. Th. Frauenheim et al., J. Phys.: Condens. Matter **14**, 3015 (2002).
56. E. N. Voronina and L. S. Novikov, Bull. Russ. Acad. Sci.: Phys. **77**, 814 (2013).
57. T. K. Minton and D. J. Garton, in *Chemical Dynamics in Extreme Environments,* Ed. by R. A. Dressler, Adv. Ser. Phys. Chem. **11**, 420 (2001).
58. V. N. Chernik, in *Proceedings of the 7th International Symposium on Materials in Space Environment, Toulouse, 1997,* Ed. by T. D. Guyenne, ESA-SP-399 (European Space Agency, France, Noordwijk, 1997), p. 237.
59. N. G. Chechenin, P. N. Chernykh, E. A. Vorobyeva, and O. S. Timofeev, Appl. Surf. Sci. **275**, 217 (2013).
60. L. S. Novikov, E. N. Voronina, V. N. Chernik, N. G. Chechenin, A. V. Makunin, and E. A. Vorob'eva, J. Surf. Invest.: X-Ray, Synchrotr., Neutron Tech. **10**, 617 (2016).
61. L. S. Novikov, E. N. Voronina, V. N. Chernik, K. B. Vernigorov, and M. Yu. Yablokova, J. Space Rockets **53**, 1012 (2016).
62. D. V. Kosynkin, A. L. Higginbotham, A. Sinitskii, J. R. Lomeda, A. Dimiev, B. K. Price, and J. M. Tour, Nature **458**, 872 (2009).
63. E. N. Voronina and L. S. Novikov, RSC Adv. **3**, 15362 (2013).
64. E. N. Voronina, L. S. Novikov, V. N. Chernik, N. P. Chirskaya, K. B. Vernigorov, G. G. Bondarenko, and A. I. Gaidar, Inorg. Mater.: Appl. Res. **3**, 95 (2012).
65. K. B. Vernigorov, A. Yu. Alent'ev, A. M. Muzafarov, L. S. Novikov, and V. N. Chernik, J. Surf. Invest.: X-ray, Synchrotr., Neutron Tech. **5**, 263 (2011).
66. L. S. Novikov, E. N. Voronina, V. N. Chernik, and L. A. Zhilyakov, J. Surf. Invest.: X-ray, Synchrotr., Neutron Tech. **10**, 829 (2016).